

# Heat Transfer Performance of a Novel Circular Flow Jet Impingement Bifacial Photovoltaic Thermal PVT Solar Collector

Muhammad Amir Aziat Bin Ishak\*<sup>ID</sup>, Adnan Ibrahim\*<sup>‡ID</sup>, Kamaruzzaman Sopian\*<sup>ID</sup>, Mohd Faizal Fauzan\*<sup>ID</sup>, Muhammad Aqil Afham Rahmat\*<sup>ID</sup>, Ag Sufiyan Abd Hamid\*\*<sup>†ID</sup>

\* Solar Energy Research Institute, Universiti Kebangsaan Malaysia, 43600, Bangi, Selangor, Malaysia

\*\* Faculty of Science and Natural Resources, Universiti Malaysia Sabah, 88400 Kota Kinabalu, Sabah, Malaysia

(amirishak93@yahoo.com, iadnan@ukm.edu.my, ksopian@ukm.edu.my, drfaizalfauzan@ukm.edu.my, immiedwardian@gmail.com, pian@ums.edu.my)

‡Adnan Ibrahim, Solar Energy Research Institute, Universiti Kebangsaan Malaysia, 43600, Bangi, Selangor, Malaysia, Tel: + 60 389118581, iadnan@ukm.edu.my

†Ag Sufiyan Abd Hamid, Faculty of Science and Natural Resources, Universiti Malaysia Sabah, 88400 Kota Kinabalu, Sabah, Malaysia, Tel; +6088 320000, pian@ums.edu.my

*Received: xx.xx.xxxx Accepted:xx.xx.xxxx*

**Abstract-** Jet impingement is commonly used to enhance the performance of solar collectors by improving the heat transfer rate. This paper presents a Novel Circular Flow Jet Impingement applied to a bifacial photovoltaic thermal (PVT) solar collector. The energy performance of the PVT solar collector was analyzed using CFD COMSOL simulation. The circular flow cup was attached to the jet plate with 36 jet plate holes and streamwise pitch,  $X = 113.4\text{mm}$ , and spanwise pitch,  $Y = 126\text{mm}$ . The inlet circular cup diameter of 6mm and outlet jet plate hole of 3mm are used to promote impinging jet effects on the photovoltaic module. The mass flow rate ranges between 0.01-0.14kg/s, and Reynolds number ranges between 2,738-14,170 to promote turbulent flow. The swirling and diffusive properties of turbulence enhance the heat transfer rate. The study was conducted to analyze two distinct scenarios: the first sought to identify the optimal diameter size, and the second sought to determine the optimal depth for the circular cup. Each model was tested with a solar irradiance ranging from 600W/m<sup>2</sup> to 900W/m<sup>2</sup>. The optimum design for the Circular Flow Jet Impingement was achieved using a 40mm diameter and 20mm depth with a maximum photovoltaic, thermal, and overall efficiency of 63%, 11.09% and 74.09% at an irradiance of 900W/m<sup>2</sup> and flow rate of 0.14kg/s.

**Keywords** Jet impingement, Photovoltaic Thermal (PVT), Heat transfer, Solar collector, CFD simulation

## 1. Introduction

The rapid expansion in worldwide consumption of energy production intensified the need for renewable energy [1]. Demand for electrical energy increases daily [2]. Solar energy is an ideal form of energy because of its abundance and accessibility—the solar cell works by taking in photons of solar irradiance and converting them into useful electrical current. Using renewable energy sources, energy efficiency and electrical consumption improvements can cumulatively result in a 94% reduction in emissions [3], [4]. Solar renewable energy is quite dependable, and its lifespan is anticipated to be between 20 to 30 years [5], [6]. In recent decades, there has been a concentrated effort within the scientific community to develop technologies capable of harnessing and transforming various forms of renewable

energy, especially solar, into usable forms of energy [7]. Renewable energy has exhibited a substantial increase in recent years [8]. It is essential to explore an alternate approach to utilize solar energy in useful forms to replace fossil fuels under the circumstances most likely to begin depleting [9]. The incorporation of renewable energy has accelerated [10]. A photovoltaic thermal (PVT) solar collector is a type of solar collector that integrates solar thermal heating and photovoltaic power generation in one system [11]. This type of solar collector combines solar photovoltaic (PV) and thermal technologies benefits. Inadvertently, the heat gain from exposure to the sun has a detrimental effect on the solar collector's efficiency. The PV panel's ability to generate useful electricity decreases when its temperature rises due to exposure to the sun [12], [13].

Solar photovoltaic thermal is a feasible source of renewable energy [14]. A PVT solar collector's performance is significantly influenced by environmental factors such as the solar irradiance [15]. An important aspect of PVT collector efficiency is the collector's cooling system [16]. Jet impingement is a technique often used to enhance the efficiency of a PVT collector by improving the heat transfer rate. The jet impingement approach, either by using a jet nozzle or jet plate, has been a primary focus of prior research to enhance or modulate heat transfer [17]. One of the passive approaches for improving heat transmission is introducing turbulent flow where fluid and heat are mixed rapidly [18]. This method is among the most common types of flows used in heat transfer applications. Research studies on convective heat transfer in both laminar and turbulent flows have reported a substantial heat transfer improvement in turbulent flow [19]–[21].

This study presents a Novel Circular Flow Jet Impingement Bifacial PVT Solar Collector to decrease the PVT system's temperature while increasing its photovoltaic and thermal efficiency. Computational Fluid Dynamics (CFD) simulation was carried out to analyze two particular scenarios: the first was to identify the optimum diameter size of the circular flow jet impingement cup, and the second was to determine the optimum depth for the circular flow jet impingement cup. CFD is a potent tool for understanding fluid flow behaviour, making it an increasingly popular choice across a broad spectrum of sectors. CFD enables the modelling of a vast array of physical and boundaries condition, which may not be viable or practical using experimental techniques. Each design of the circular flow cup was tested with a solar irradiance ranging from 600-900W/m<sup>2</sup> to find the optimum design of the circular flow jet impingement that leads to the highest performance of the PVT solar collector. The Reynolds number ranges between 2,738 – 14,170 to promote turbulent flow along the air duct. The streamwise, X=113.4 mm and spanwise, Y=126mm, distribute the air evenly across the PV module surface. The streamwise and spanwise pitch significantly influence heat transmission characteristics of jet impingement [22].

**2. Computational Analysis**

*2.1. Design Model*

Computational fluid dynamic modelling using COMSOL Multiphysics 5.6 was carried out to analyze two different cases: the optimum diameter size of the Circular Flow cup and the optimum Circular Flow cup depth. The Circular Flow cup air inlet is set to 6mm with an outlet jet plate hole of 3mm to promote impinging jet effects while increasing the air velocity. The Circular Flow cup is attached at the back of a jet plate consisting of 36 jet plate holes and streamwise pitch, X = 113.4mm, and spanwise pitch, Y= 126mm. The PVT collector's dimension is L= 705mm, W= 684, and duct depth, d = 25mm. The parameters and based value can be referred at Table 3. The number of jet holes and the streamwise and spanwise value is chosen as it has been proven to achieve a maximum photovoltaic and thermal efficiency of 10.69% and 51.09% at solar irradiance of 900W/m<sup>2</sup> [23]. A circular flow

cup diameter of 40mm, 50mm, and 60mm, as shown in Fig. 1, is used to find the optimum diameter size of the Novel Circular Flow Jet Impingement Photovoltaic Thermal (PVT). Thus, each model is simulated using a mass flow rate between 0.01-0.14kg/s and heat flux between 600-900W/m<sup>2</sup>.

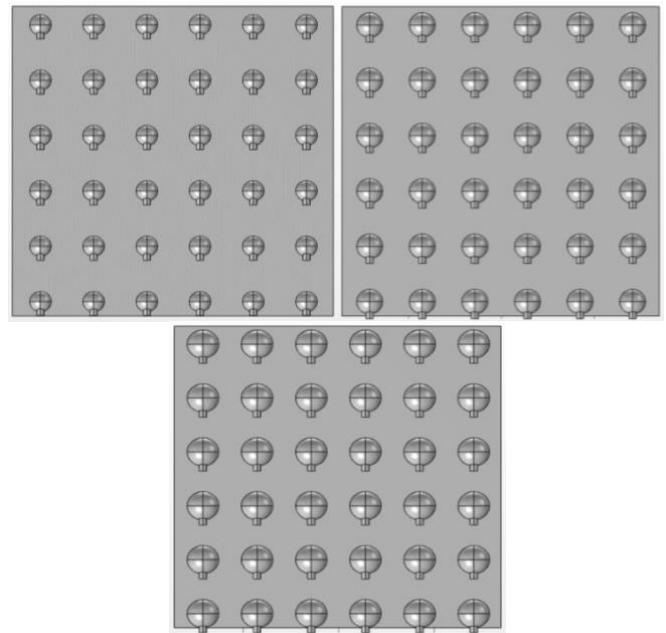


**Fig. 1** Back view of Circular Flow cup attached at the back of the jet plate: from left 40mm, 50mm, and 60mm cup diameter.

*2.2. Mesh Independent Study*

The Novel Circular Flow Jet Impingement Bifacial PVT Solar Collector geometry model was rendered with nine different meshings, starting from the lowest to the highest, as shown in Fig. 2. The number of elements and average element quality for each mesh setup were analyzed to differentiate the quality and accuracy between the meshing types, as shown in Table 1. Mesh independent study is performed to allow the numerical output to achieve the highest level of accuracy.

**Table 1** The number of elements and the average element quality for each mesh setting.

Mesh	No of Element	Average Element Quality	Difference in Average Element Quality
Extremely coarse	488,094	0.578	4.38%
Extra coarse	1,219,511	0.622	1.42%
coarser	1,375,958	0.636	1.87%
coarse	2,221,555	0.655	2.26%
normal	5,566,743	0.677	1.22%
fine	16,983,249	0.689	0.22%
finer	79,613,812	0.692	-0.32%
extra fine	98,763,462	0.688	-0.78%
extremely fine	178,316,508	0.681	

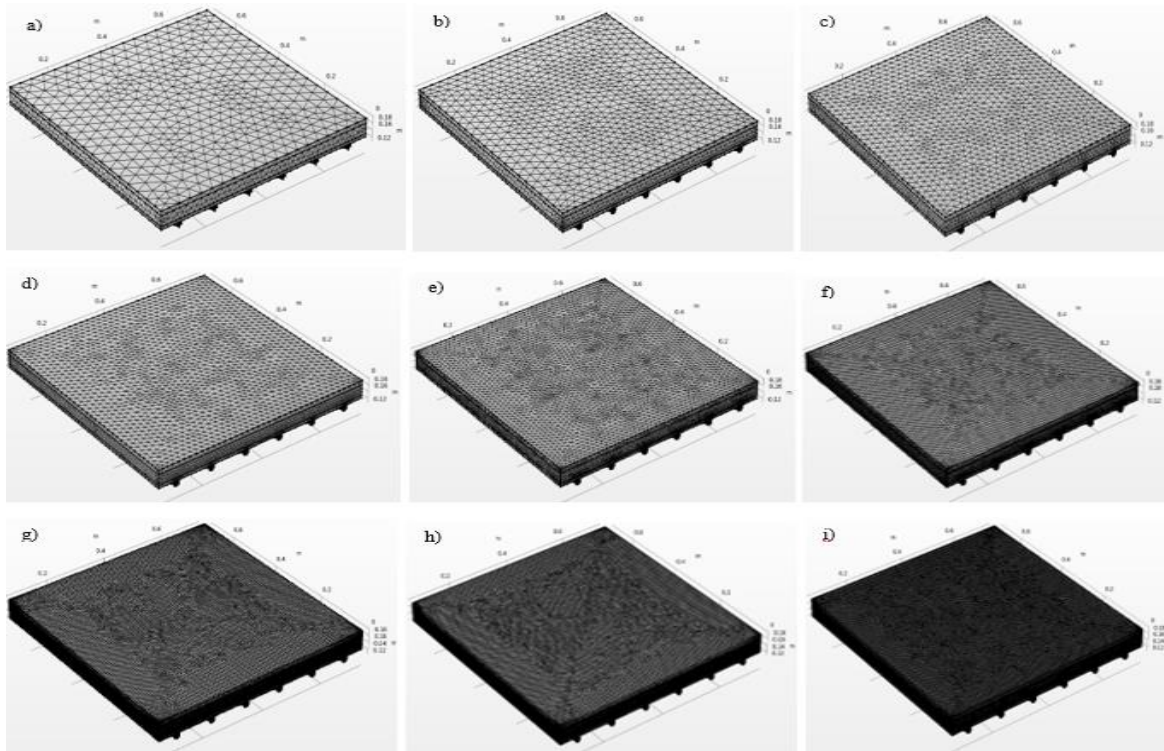


**Fig. 2** Different mesh settings starting from top left a) extremely coarse, (b) extra coarse, (c) coarse, (d) coarser, (e) normal, (f) fine, (g) finer, (h) extra fine and (i) extremely fine.

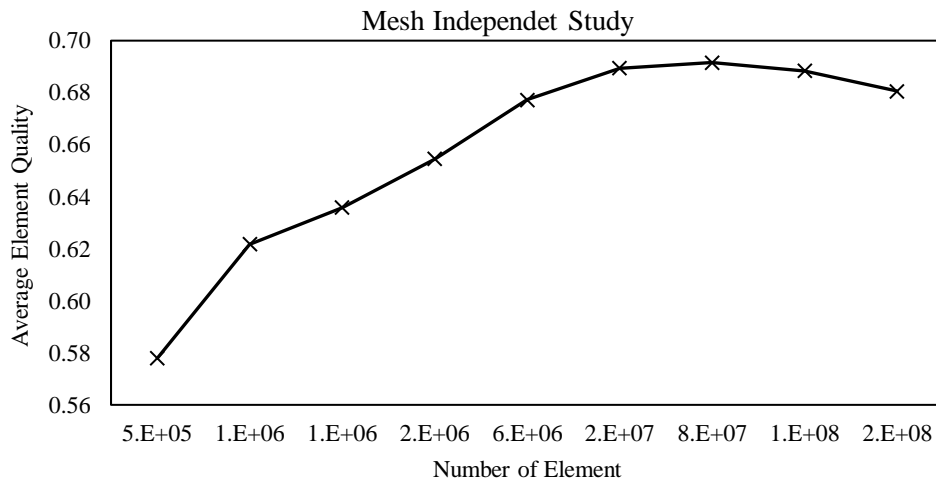


**Fig. 3** Mesh independent study analysis for the number of elements against average element quality.

The independent mesh study was conducted starting from extremely coarse, the most-coarse element of the mesh settings, up to extremely fine, which is the highest and finest rendering. The elements range from 488,094 to 178,316,508, and the average element quality ranges from 0.578 to 0.681. The difference percentage between the average element quality decrease from extremely coarse to fine mesh settings. However, when finer mesh settings are used, the difference percentage reaches a negative value of -0.38%. This indicates that using meshing beyond finer settings doesn't have a significant effect. It can also be observed that from Fig. 3,

Finer mesh settings have the highest average element quality, which is 0.692. Thus, finer mesh settings are used in computational modelling.

*2.3. Validation of Model*

Using the same simulation boundary conditions and settings developed, modelling from Win Eng Ewe et al. 2021 [23] and experimental results from Win Eng Ewe et al. 2022 [24] were carried out. Model validation is performed in COMSOL to evaluate the reliability of the simulation model

settings by comparing them with previous studies. Fig. 4 presents the findings obtained under similar operational circumstances and design settings:  $\dot{m}=0.014\text{-}0.035\text{kg/s}$ ,  $W=0.684\text{m}$ ,  $L=0.705\text{m}$ , and  $d=0.025\text{m}$ . For comparison, only

the overall efficiency is calculated between the past and current studies. The average accuracy percentage in the previous modelling study was 97.73%, while compared to the previous experimental was 94.33%, as shown in Table 2.

**Table 2** Simulation configuration accuracy by comparing overall efficiency between previous studies.

Overall Efficiency (%)							
mass flow rate (kg/s)	(Ewe Wing Eng et al. 2021) Model	Current Work	Error (%)	(Ewe Wing Eng et al., 2022) Experiment	Current Work	Error (%)	
0.014	51.51	52.57	2.02	50.16	52.57	4.59	
0.016	53.44	54.5	1.95	51.31	54.5	5.86	
0.018	55.11	56.42	2.32	52.68	56.42	6.62	
0.025	59.49	61.01	2.49	57.09	61.01	6.42	
0.035	63.48	65.16	2.58	61.99	65.16	4.87	
Average percentage error (%)			2.27%	Average percentage accuracy (%)			94.33%
			97.73%				

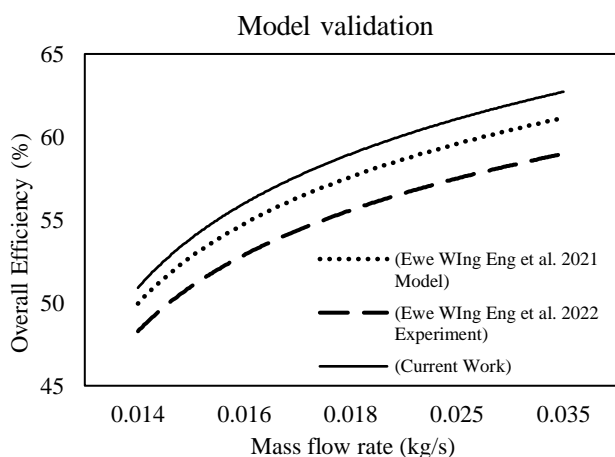


**Fig. 4** Model validation of simulated thermal efficiency compared to current work

**2.4. Parameters and Boundary Conditions**

Temperature-dependent characteristics in COMSOL Multiphysics allow the analysis of fluid domain properties such as air and fluid and solid domain properties such as aluminium, steel, and other materials simultaneously. Several assumptions were made before the simulation, including that the thermal configurations of PVT collector components such as laminations, jet plate reflectors, and PV cells are neglected. Second, no air leakage occurs along the collector's path, and no heat is lost at the collector's edges. Lastly, the bifacial PV module front and back surfaces are at equal temperatures. In conjugate heat transfer with turbulent flow, the  $k-\epsilon$  interface is employed to analyze the correlations between heat transfer in fluid flow and heat transfer in solids. Turbulent flow,  $k-\epsilon$ , is selected based on the Reynolds number that can be referred to in subsection 2.4.1 Reynolds number. The Reynolds-averaged Navier-stokes (RANS) is utilized in the simulation to solve the turbulent flow. Non-isothermal flow coupling between the turbulent flow  $k-\epsilon$  and heat transfer in solid and fluid is added. The reference temperature,  $T_{ref}$ , is set to 303.15 K. Heat flux

of  $600\text{-}900\text{W/m}^2$  is tested for each mass flow rate range from  $0.01\text{-}0.14\text{kg/s}$ . Convective heat flux was also included where the heat transfer coefficient,  $h$ , was set to  $9\text{W/m}^2\cdot\text{K}$  and the external temperature  $T_{ext}$  was  $30^\circ\text{C}$ . The PV panel's surface-to-ambient radiations were added with a surface emissivity,  $\epsilon$  of 0.95. Table 3 presents the parameter and base value used in the simulation.

**Table 3** Parameters and base value

Parameter	Value
Mass flow rate, $\dot{m}$	0.1 – 0.14 kg/s
Width of collector, $W$	684mm
Length of collector, $L$	705mm
Duct Depth, $d$	25mm
Solar irradiance, $I$ ( $\text{W/m}^2$ )	600, 700, 800, 900
Area of collector, $A_c$	$0.481\text{m}^2$
Temperature ambient, $T_a$	$30^\circ\text{C}$
Absorptivity of PV cell, $\alpha_{pv}$	0.91
Packing factor, $P$	0.66
Heat transfer coefficient, $h$	$9\text{W}/(\text{m}^2\cdot\text{K})$
External temperature, $T_{ext}$	$30^\circ\text{C}$
Transmittance of Lamination, $\tau_1$	0.85
Reflectivity of jet plate, $n_R$	0.7
Electrical efficiency at reference condition, $\eta_{ref}$	0.16
Temperature Coefficient, $\beta$	$0.0045\text{K}^{-1}$
Temperature at reference condition, $T_{ref}$	$303.15\text{K}$

**2.4.1. Reynolds Number**

The Reynolds number determines the airflow inside the Novel Circular Flow Jet Impingement Bifacial PVT Solar Collector. Based on the formula below, the Reynolds number ranges between 2,738 – 14,170. The mass flow rate range between  $0.01\text{-}0.14\text{kg/s}$ . Therefore, Turbulent conjugate heat transfer settings are used in the CFD COMSOL. Conjugate heat transfer uses an analysis combination between heat transfer and fluid flow.

The Reynolds number,  $Re$ , is calculated by using [25]:

$$\text{Reynolds number} = \frac{\dot{m} Dh}{W d \mu} \quad (1)$$

Where hydraulic diameter,  $Dh$ , is calculated by using [24]:

$$Dh = \frac{4 W d}{2 (W + d)} \quad (2)$$

And viscosity of air is calculated by using [24]:

$$\mu = [1.983 + 0.00184 (T - 300)] \times 10^{-5} \quad (3)$$

2.4.2. Convective Heat Flux

The convective heat flux,  $q_0$ , is given by:

$$q_0 = h. (T_{ext} - T) \quad (4)$$

2.4.3. Thermal Efficiency

Thermal efficiency,  $\eta_{thermal}$  of the PVT collector is expressed as [24]:

$$\eta_{thermal} = \frac{Qu}{(I \times Ac)} \quad (5)$$

Where useful heat gain,  $Qu$ , is calculated using:

$$Qu = \dot{m} C_p (T_a - T_i) \quad (6)$$

2.4.4. Photovoltaic Efficiency

Photovoltaic efficiency,  $\eta_{elec}$  of the system is calculated using:

$$\eta_{elec} = \frac{P_{max}}{(I \times Ac)} \quad (7)$$

Since the system uses a Bifacial solar cell, the maximum power,  $P_{max}$ , is calculated using [26]:

$$P_{max} = I A_c \alpha_{pv} P (\eta_{pvfront}) + I A_c \tau_i (1 - P) n_r \alpha_{pv} P (\eta_{pvfront}) \quad (8)$$

Where the efficiency of the cell is given by [27]:

$$\eta_{pvfront} = \eta_{pvrear} = \eta_{ref} [1 - \beta (T_{pv} - T_{ref})] \quad (9)$$

2.4.5. Overall Efficiency

The overall efficiency of the PVT collector can be expressed as follows:

$$\eta_{overall} = \eta_{photovoltaic} + \eta_{thermal} \quad (10)$$

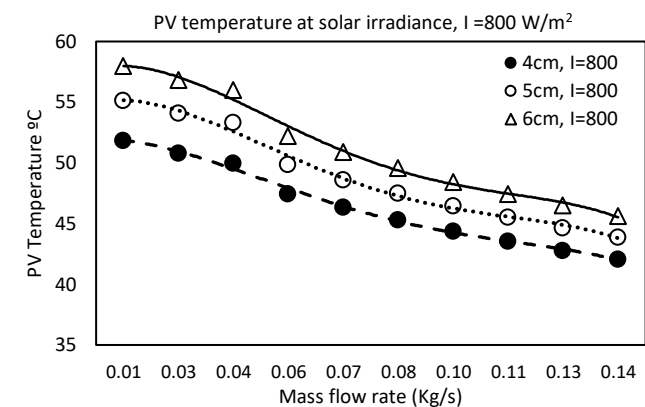
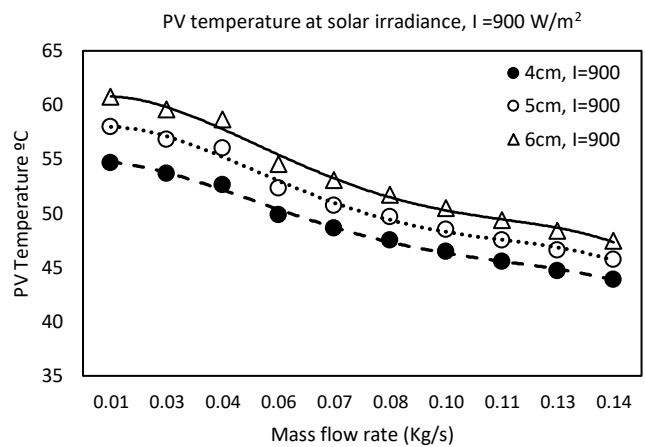
3. Results and Discussions

The heat transfer performance of the Novel Circular Flow Jet Impingement Bifacial PVT Solar Collector is assessed based on the photovoltaic, thermal, and overall efficiency of the PVT collector. The result is divided into two subsections: the effects of the diameter size on the collector's efficiency and the effects of depth size on the collector's efficiency.

3.1. Effects of Diameter Size on The Collector's Efficiency

3.1.1. Photovoltaic Efficiency

The PV module temperature in Fig. 5 shows a downtrend for all three-diameter sizes. The PV temperature drops as the mass flow rate and solar irradiance increase. Referring to equation (7), the PV temperature and solar irradiance are directly proportional to the photovoltaic efficiency. Hence, lowering the PV module temperature can improve the photovoltaic efficiency. Based on Fig. 5, a 40mm diameter has the lowest PV temperature compared to 50mm and 60mm diameters. The lowest PV temperature recorded was at 600W/m<sup>2</sup> at a mass flow rate of 0.14kg/s which 40mm achieved a reading of 38.32°C. Under the same operating conditions, 50mm and 60mm PV temperature was 40.17°C and 41.95°C. At the highest solar irradiance of 900W/m<sup>2</sup>, the lowest PV temperature for 40mm, 50mm, and 60mm was 43.9°C, 45.73°C, and 47.45°C at a mass flow rate of 0.14kg/s.



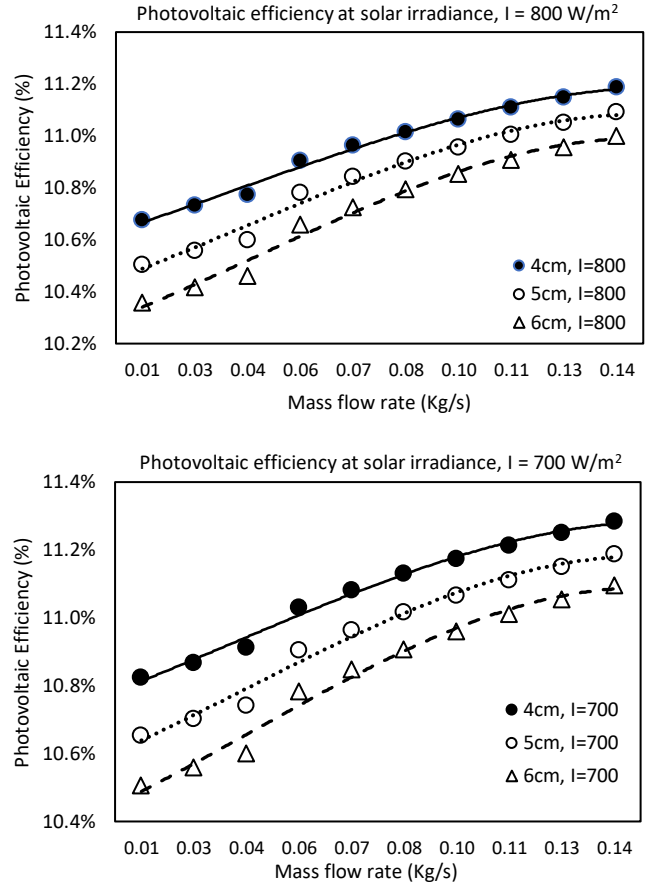
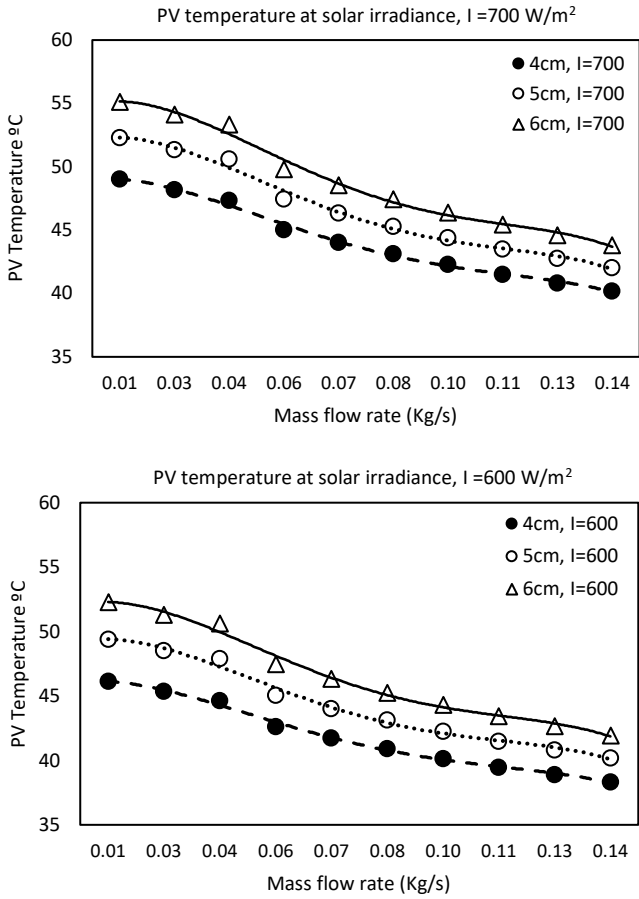


**Fig. 5** PV temperature of 40mm, 50mm, and 60mm diameter cup.

The photovoltaic efficiency increases as the mass flow rate increases while solar irradiance drops. This is proven as shown in Fig. 6. In comparison, 40mm has the highest photovoltaic efficiency among the three diameter sizes. The maximum thermal efficiency achieved with 40mm was 11.38% at 600W/m² and the mass flow rate was 0.14kg/s, while 50mm and 60mm gained a maximum photovoltaic efficiency of 11.28% and 11.19% under the same conditions. At the highest solar irradiance of 900W/m² tested, the photovoltaic efficiency for 40mm, 50mm, and 60mm was 11.09%, 11%, and 10.91%, respectively.

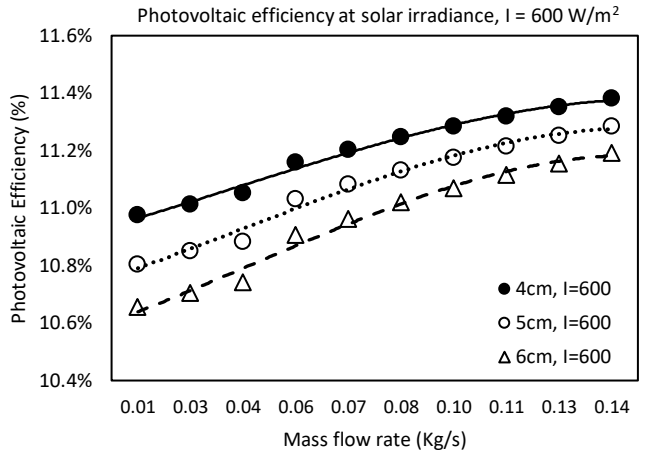
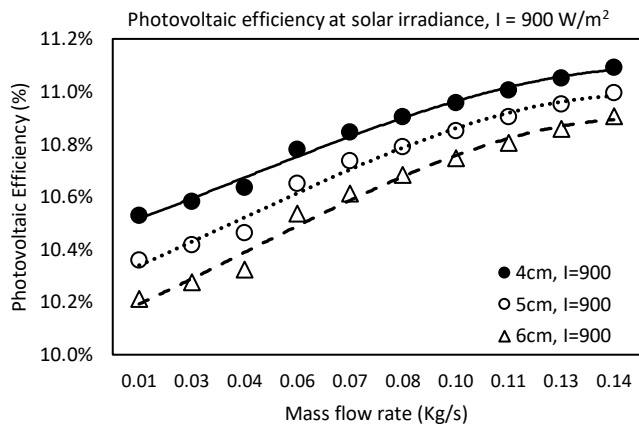


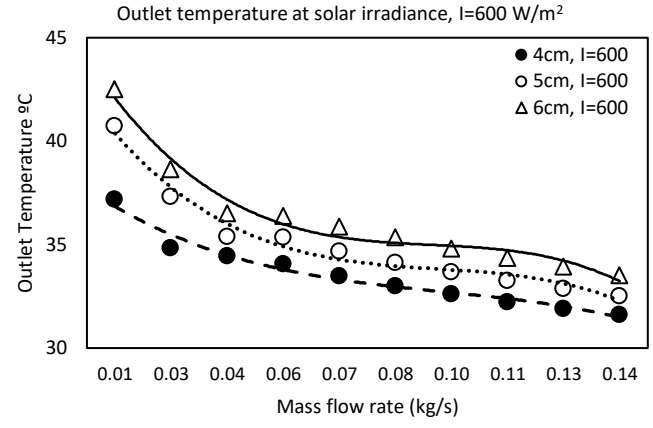
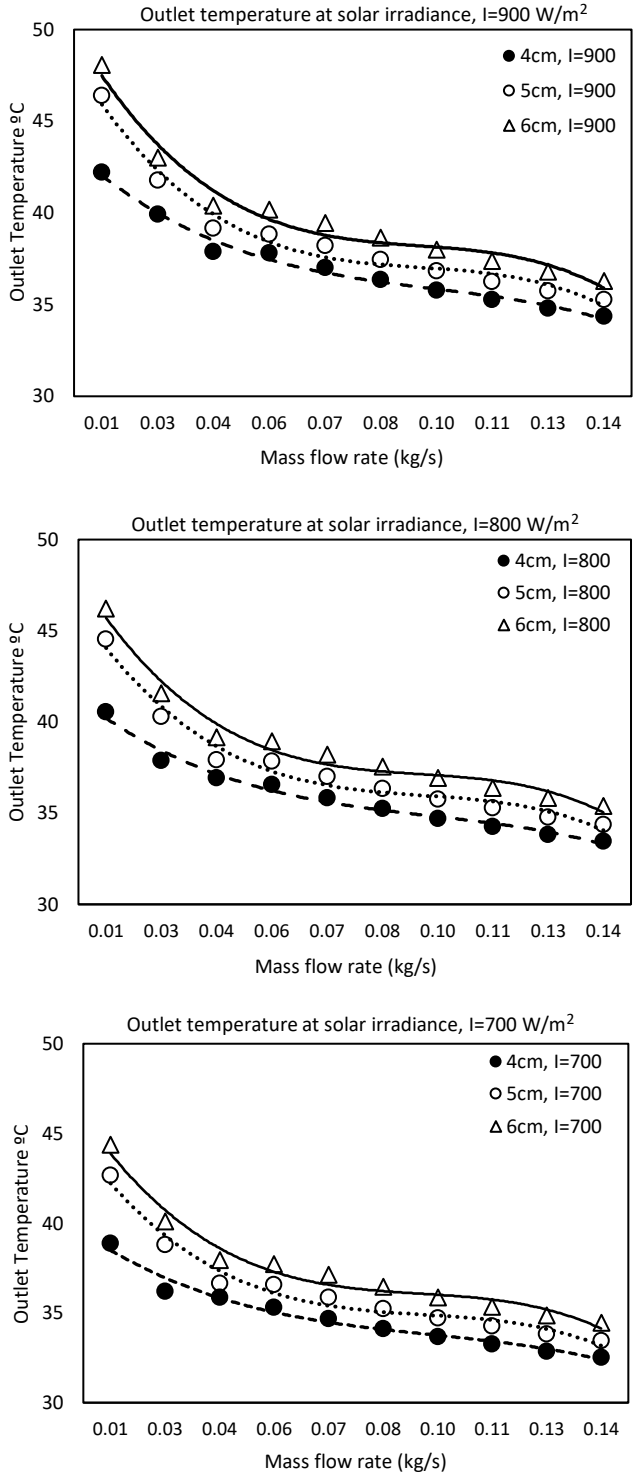
**Fig. 6** Photovoltaic efficiency of 40mm, 50mm, and 60mm diameter cups.



3.1.2. Thermal Efficiency

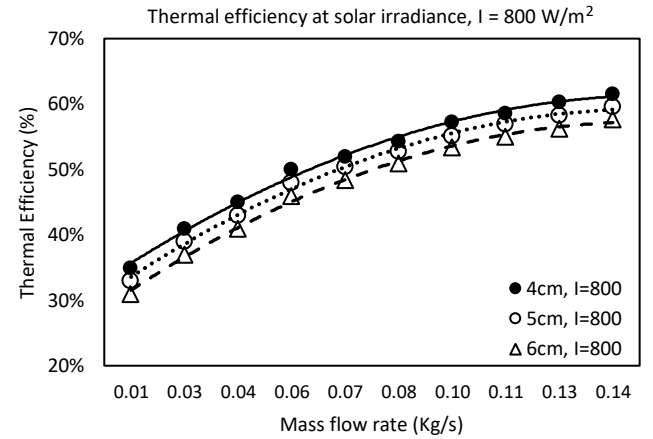
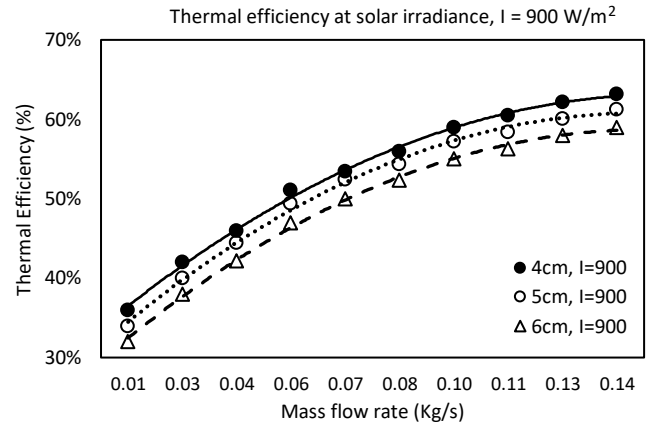
The outlet temperature was measured at variable solar irradiance, from 600, 700, 800, and 900W/m² for each mass flow rate. A downtrend in the outlet temperature can be observed in Fig. 7 as the mass flow rate increases for all circular cup diameter sizes. However, for all solar irradiance tested, the 40mm diameter size has the lowest outlet temperature compared to 50mm and 60mm. The lowest outlet temperature recorded was 31.61°C with a 40mm diameter at solar irradiance 600W/m² and a mass flow rate of 0.14kg/s. The 60mm diameter has the highest outlet temperature for all

solar irradiance recorded, with the highest reading of 48.08°C at 900W/m<sup>2</sup> and a mass flow rate of 0.01kg/s. At the highest solar irradiance tested, 900W/m<sup>2</sup>, and mass flow rate of 0.14kg/s, the outlet temperature recorded for 40mm, 50mm, and 60mm diameter was 34.37°C, 35.29°C, and 36.3°C respectively. When tested with the lowest solar irradiance of 600W/m<sup>2</sup> at a mass flow rate of 0.14kg/s, the 40mm, 50mm, and 60mm outlet readings were 31.61°C, 32.54°C, and 33.54°C.



**Fig. 7** Outlet temperature of 40mm, 50mm, and 60mm diameter cup.

It was observed in Fig. 8 that the thermal efficiency is directly proportional to the mass flow rate. The thermal efficiency improves as the mass flow rate increases. 40mm diameter recorded the highest thermal efficiency of 63% at solar irradiance 900W/m<sup>2</sup> and mass flow rate of 0.14kg/s. Meanwhile, under the same operating conditions, the maximum thermal efficiency for 50mm and 60mm diameters was 61% and 59%. The lowest thermal efficiency recorded was at 600W/m<sup>2</sup> at a mass flow rate of 0.01kg/s with a 60mm diameter with the weakest reading of 29%, followed by 50mm, 31%, and 40mm, 33%.



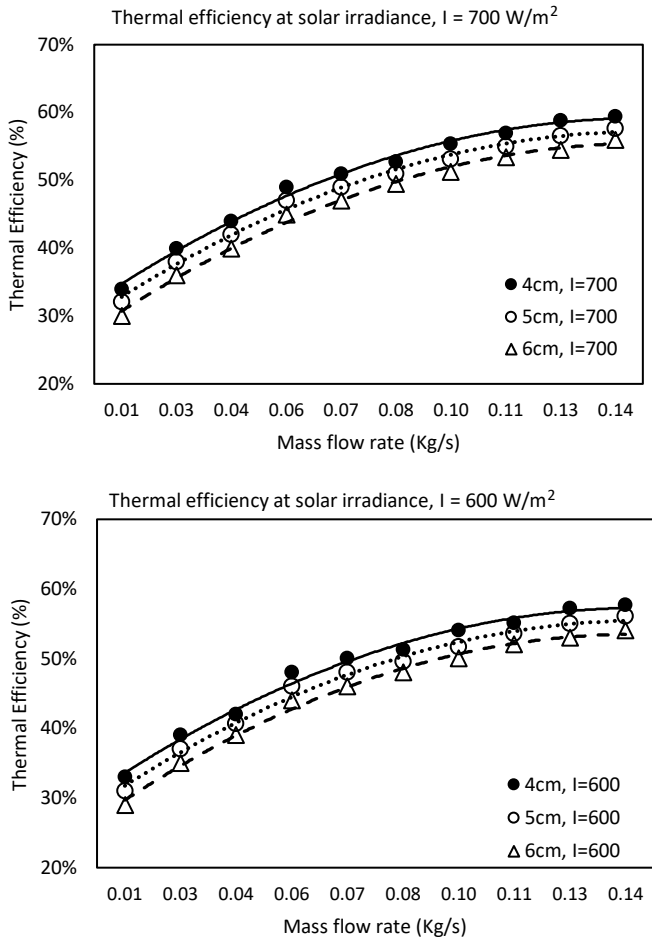


**Fig. 8** Thermal efficiency of 40mm, 50mm, and 60mm diameter cup.

3.2. Effect of Depth Size on The Collector's Efficiency

Based on subsection 3.1, the optimum diameter size for the circular cup was 40mm, with the highest photovoltaic and thermal efficiency was 11.09% and 63% at the highest solar irradiance of  $900 \text{ W/m}^2$ . After the optimum diameter size was achieved, the depth size of the circular cup was analyzed to evaluate the effects of depth size on the collector's performance. The same procedure and boundary conditions are implemented using 20mm, 30mm, 40mm, and 50mm depth.

3.2.1. Photovoltaic Efficiency

In Fig. 9, it can be observed that increasing the mass flow rate will make the PV temperature drop. It is due to the heat transfer rate increasing with increasing mass flow rate. Thus, another factor contributes to the PV drop in solar irradiance. However, the PV temperature is simulated at a maximum of  $900 \text{ W/m}^2$  to observe the maximum performance achieved under high solar irradiance. At solar irradiance of  $600 \text{ W/m}^2$ , the PV temperature range for 20mm, 30mm, 40mm, and 50mm depth was  $46.13\text{-}38.32^\circ\text{C}$ ,  $49.03\text{-}40.17^\circ\text{C}$ ,  $52.32\text{-}41.98^\circ\text{C}$  and  $54.13\text{-}43.29^\circ\text{C}$  for mass flow rate from 0.01 to  $0.14 \text{ kg/s}$ . At the highest solar irradiance of  $900 \text{ W/m}^2$ , the PV

temperature ranges from  $54.69\text{-}43.9^\circ\text{C}$  for 20mm depth,  $57.5\text{-}45.71^\circ\text{C}$  for 30mm depth,  $59.81\text{-}47.5^\circ\text{C}$  for 40mm depth and  $61.58\text{-}49.48^\circ\text{C}$ .

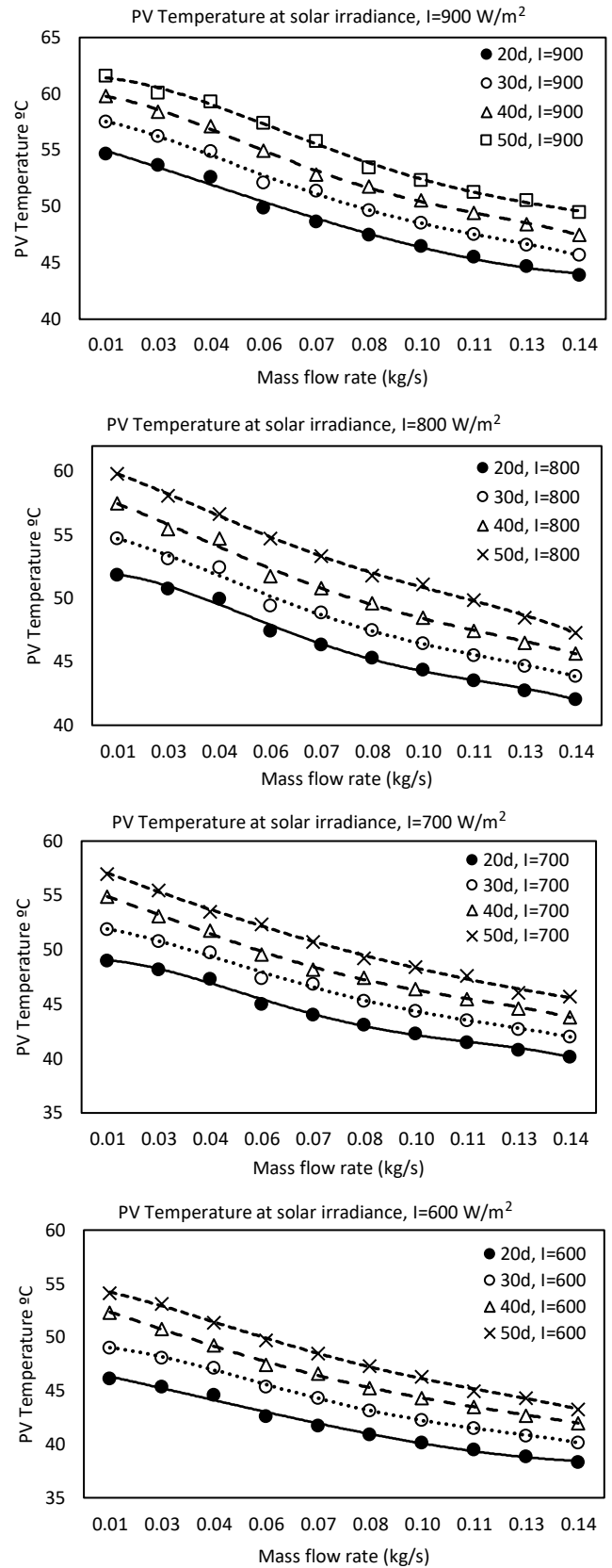


**Fig. 9** PV temperature of 20mm, 30mm, 40mm, and 50mm circular cup depth

The chart in Fig. 10 shows that the photovoltaic efficiency increases as the mass flow rate increases. An increased mass flow rate results in a quicker heat transfer rate in the PVT collector. In addition to improving photovoltaic efficiency, the PV panel's ability to operate at lower temperatures increases energy production. However, when exposed to increasing solar irradiance, the PV temperature rises because the solar collector absorbs more heat. Thus, the photovoltaic efficiency will decrease when the PVT collector is exposed to high temperatures. Based on Fig. 10, 20mm depth has the highest photovoltaic efficiency compared to other depth sizes. The maximum photovoltaic efficiency recorded by 20mm depth was 11.38% at 600W/m<sup>2</sup> and mass flow rate of 0.14kg/s. Under the same operating conditions, the 30mm, 40mm, and 50mm depth sizes recorded a maximum photovoltaic efficiency of 11.28%, 11.19%, and 11.12%.

Meanwhile, when tested at the highest solar irradiance of 900W/m<sup>2</sup>, the highest photovoltaic efficiency recorded was by using a 20mm depth with a photovoltaic efficiency ranging from 10.53-11.09%. The photovoltaic efficiency for the 30mm, 40mm and 50mm under the same operating condition ranges from 10.53-11.09%, 10.38-11%, 10.26-10.90%, and 10.17-10.80%, respectively. Overall, the 20mm depth size recorded the highest photovoltaic efficiency at all solar irradiance tested compared to other depth sizes. The depth size of the circular flow jet impingement affects the performance of the PVT solar collector efficiency. When the depth size increases, the PV temperature also increases due to the turbulent effects starting to decrease as the air circulates in the cup and takes longer time to leave the jet plate. This situation is illustrated in the streamline section, which demonstrates the air velocity streamline in the circular flow jet impingement cup.

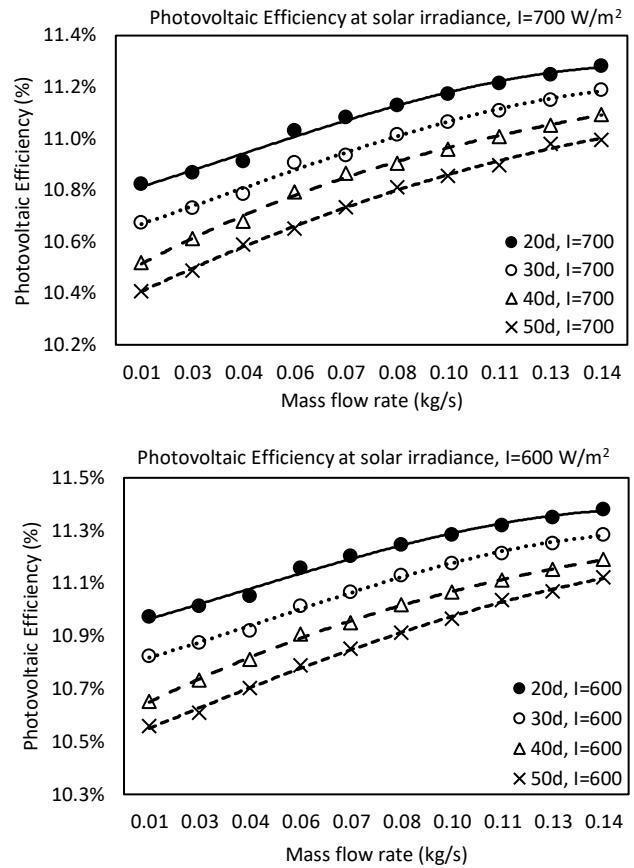
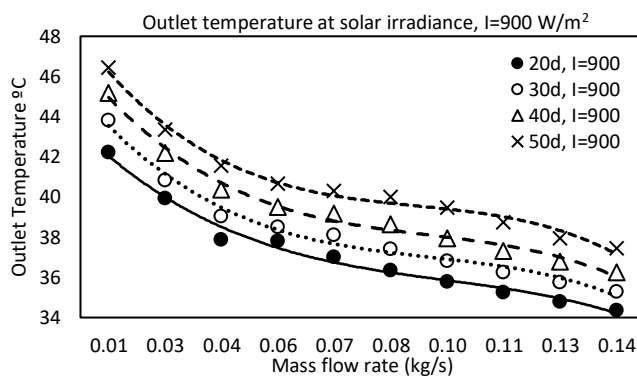
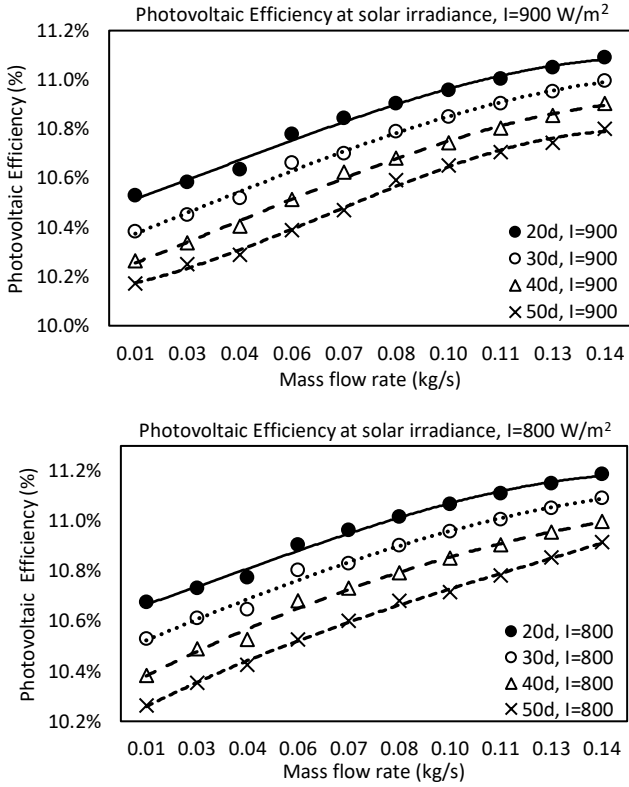
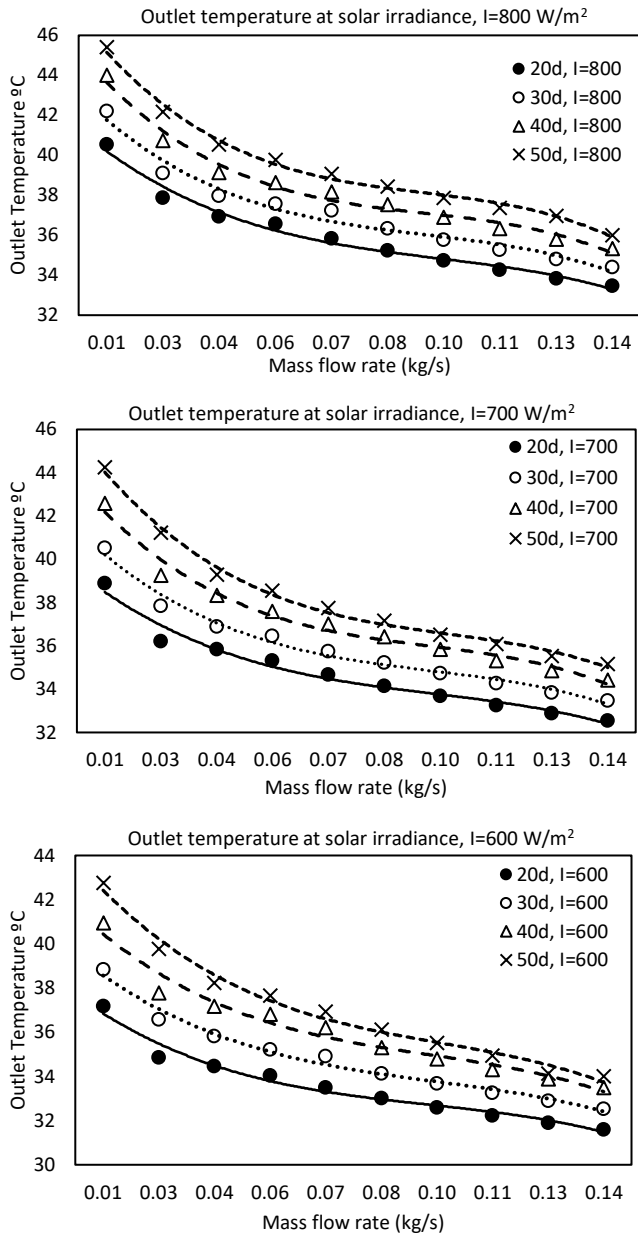


Fig. 10 Photovoltaic efficiency of 20mm, 30mm, 40mm, and 50mm circular cup depth.

3.2.2. Thermal Efficiency

From Fig. 11, it can be observed that the outlet temperature increases as the depth of the circular cup increases. The depth of the circular cup varies from 20mm, 30mm, 40mm, and 50mm using the optimum diameter of 40mm. The outlet temperature increases at 20mm, 30mm, 40mm, and 50mm. At a solar irradiance of 900W/m<sup>2</sup>, the highest outlet temperature recorded was 50mm at 46.45°C, 40mm at 45.19°C, 30mm at 43.83°C, and 20mm at the lowest outlet temperature at 42.22. The outlet decreases as the solar irradiance decreases and the mass flow rate increases. The lowest outlet temperature can be achieved using 600W/m<sup>2</sup> where the maximum outlet temperature for 20mm, 30mm, 40mm, and 50mm is 37.19°C, 38.86°C, 40.95 °C, and 42.76°C.





**Fig. 11** The outlet temperature of 20mm, 30mm, 40mm, and 50mm circular cup depth

The maximum thermal efficiency can be achieved with the highest solar irradiance of  $900 \text{ W/m}^2$  and a mass flow rate of  $0.14 \text{ kg/s}$ . Based on Fig 12, 20mm depth has the highest thermal efficiency compared to other depth sizes for all solar irradiance tested. The maximum thermal efficiency of 20mm depth was 63% at solar irradiance of  $900 \text{ W/m}^2$  and mass flow rate of  $0.14 \text{ kg/s}$ . Meanwhile, with the same operating conditions, 30mm, 40mm, and 50mm thermal efficiency achieved was 62%, 61%, and 60%. A slight decrement in the thermal efficiency as the depth size increases. However, when operating at  $600 \text{ W/m}^2$ , the maximum thermal efficiency achieved was 56% using 2mm depth, and the lowest thermal efficiency achieved was 29% with 50mm depth at a mass flow rate of  $0.01 \text{ kg/s}$ . When exposed to increases solar irradiance, the outlet temperature rises as the collector absorbs more heat. As a result, the thermal efficiency increases as the outlet temperature rises.

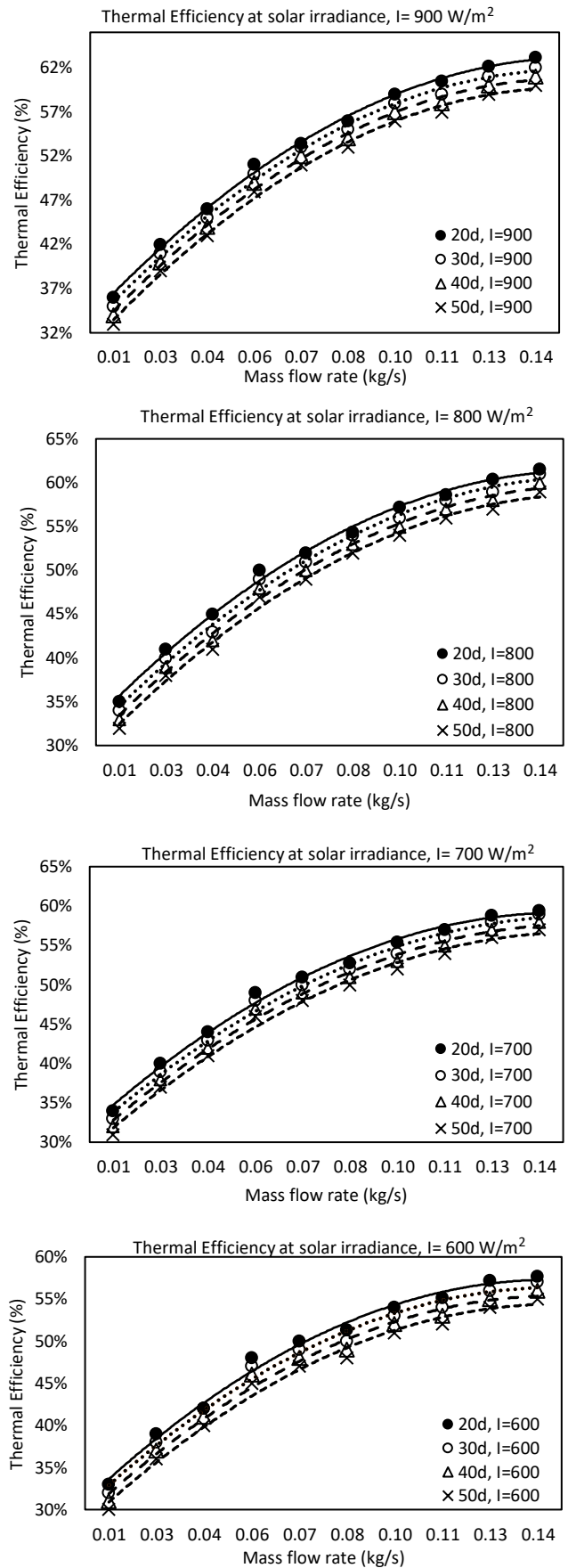


**Fig. 12** Thermal efficiency of 20mm, 30mm, 40mm, and 50mm circular cup depth.

3.2.3. Streamline

Based on Fig. 13, the air velocity in the 20mm depth cup circulates in the cup before entering the air duct between the PV module and the jet plate. The circular flow in the cup impinges on the PV module as it leaves the 3mm jet plate holes with high-velocity pressure and helps promote turbulent effects. The swirling and diffusive properties of turbulent flow enhance heat transmission. Additionally, mixing brought on by turbulent flow can prevent boundary layer development on the heat transfer core surface. It is more apparent that the heat transfer rate increases in turbulent flow than in laminar flow settings. This is because in turbulent flow, the Reynolds number of the fluid being moved increases, making the fluid more resilient. When the depth size increases, the turbulent effect starts to decrease as the air circulates in the cup and takes longer to leave. Turbulent flow can significantly effects the heat transfer rate. The existence of eddies and vortices in a fluid indicates turbulent flow, which can lead to increased mixing and hence a higher heat transfer rate. In contrast to laminar flow, the fluid is moving in a flat, parallel motions causing a boundary layer to form around the hot surface in laminar flow. This boundary layer has the potential to insulate, hence decreasing the heat transfer rate. However, in turbulent flow, the boundary layer is constantly being mixed and disrupted by the fluid, leading to increase heat transfer rate. The effects of the flow circulation in the cup can be seen in Fig. 13 and Fig. 14. As seen in Fig. 14, the air circulation streamlines in the cup are longer as the circular cup loses its circular shape as the depth increases. As a result, the air circulation effects take a long time and more pressure loss in the air velocity. Thus, the air enters the air duct at a lower speed, and the turbulent effect is lesser. Therefore, it is quite crucial to maintain the round circular shape and depth of the circular cup flow as it will affect the airflow characteristic.

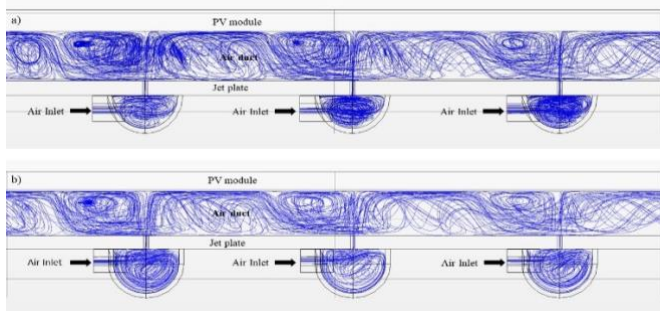


Fig. 13 Streamline for (a) 20mm depth and (b) 30mm depth.

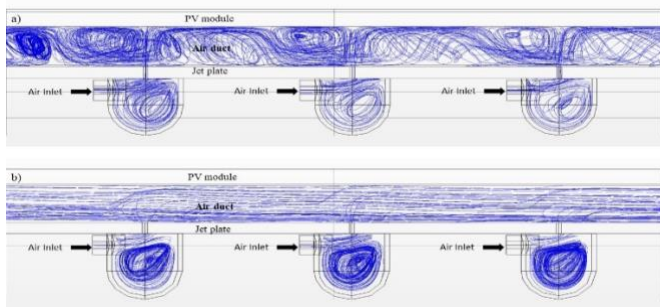


Fig. 14 Streamline for (a) 40mm depth and (b) 50mm depth.

3.3. Overall Efficiency of The Optimum Design

Based on the result, the optimum diameter and depth size for the Novel Circular Flow Jet Impingement Bifacial PVT Solar Collector was 40mm in diameter with 20mm depth. This configuration increases the PVT collector's performance and contributes to the highest photovoltaic and thermal. The overall efficiency of the optimum Circular Flow Jet Impingement can be referred to in Fig. 15. At the highest solar irradiance of 900W/m<sup>2</sup>, the maximum photovoltaic and thermal efficiencies were 11.09% and 63% with an overall efficiency of 74.28%. Meanwhile, when operating at the lowest solar irradiance of 600W/m<sup>2</sup>, the maximum photovoltaic, thermal, and overall efficiency was 11.38%, 58%, and 69.02%.

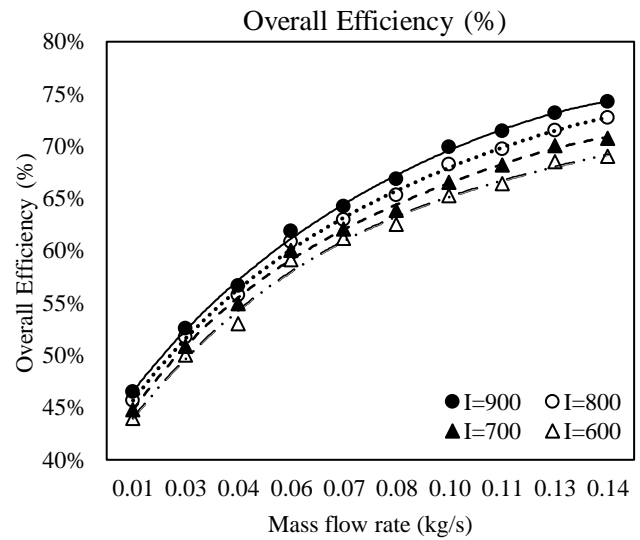


Fig. 15 Overall Efficiency for 40mm diameter with 20mm depth

4. Conclusion

This study presents a Novel Circular Flow Jet Impingement Bifacial Photovoltaic Thermal PVT Solar Collector. The circular flow cup's diameter, size, and depth influence the PVT Solar Collector's heat transfer characteristics and performance. 40mm circular cup has the highest photovoltaic and thermal efficiency compared to 50mm and 60mm diameters. At 600W/m<sup>2</sup>, the 40mm diameter photovoltaic and thermal efficiency ranges from 10.97-11.38% and 33%-58%. When operating at the highest solar irradiance of 900W/m<sup>2</sup>, the maximum photovoltaic efficiency achieved was 11.09%, while the thermal efficiency was 11.09%. After the optimum diameter of the circular cup was determined, the optimum depth of the circular flow cup was analyzed to finalize the optimum design for the circular cup to perform at its highest performance and efficiency. The optimum depth of the circular cup was 20mm, achieving the highest thermal and photovoltaic efficiency compared to 30mm, 40mm, and 50mm. When the Circular cup depth increases, the air velocity tends to circulate longer in the cup before leaving the jet plate, causing the impinging effect to decrease. The turbulent effect also decreases as the circular depth increases, as shown in Fig. 14. Therefore, a 40mm

diameter and 20mm depth combination is the optimum size for the circular flow to perform effectively. For the circular flow to perform efficiently, the semi-spherical form must be maintained so that the air velocity can circulate effectively, encouraging impinging effect and turbulent flow that enhances the heat transfer rate. The overall efficiency when operating at 900W/m<sup>2</sup> was 74.28%, while at the lowest solar irradiance tested at 600W/m<sup>2</sup> was 69.02%.

### Acknowledgements

The authors would like to acknowledge the Ministry of Higher Education of Malaysia under the Fundamental Research Grant Scheme (FRGS/1/2019/TK07/ UKM/02/4) and the Faculty of Science and Natural Resources, Universiti Malaysia Sabah (UMS) under SPBK-UMS phase 1/2022 (SBK0518-2022) (UMS) research grants.

### References

- [1] T. M. Tawfik, M. A. Badr, O. E. Abdellatif, H. M. Zakaria, and M. EL-Bayoumi, "Techno-Enviro-Economic Evaluation for Hybrid Energy System Considering Demand Side Management," *Int. J. Renew. Energy Res.*, vol. 12, no. 2, pp. 623–635, 2022, doi: 10.20508/ijrer.v12i2.12805.g8449.
- [2] Sadullah Esmer, "Design of PMaSynRM for Flywheel Energy Storage System in Smart Grids," vol. 6, no. 4, pp. 0–7, 2022.
- [3] Muhammad Aqil, Afham Rahmat, Ag Sufiyan, Abd Hamid, Yuanshen Lu, Muhammad Amir, Aziat Ishak, Shaikh Zishan Suheel, Ahmad Fazlizan, and Adnan Ibrahim, "An Analysis of Renewable Energy Technology Integration Investments in Malaysia Using HOMER Pro," 2022.
- [4] Mita Bhattacharya, Sudharshan Reddy Paramati, Ilhan Ozturk, and Sankar Bhattacharya, "The effect of renewable energy consumption on economic growth: Evidence from top 38 countries," *Appl. Energy*, vol. 162, pp. 733–741, 2016, doi: 10.1016/j.apenergy.2015.10.104.
- [5] Adnan Ibrahim, Mohd Yusof Othman, Mohd Hafidz Ruslan, Sohif Mat, and Kamaruzzaman Sopian, "Recent advances in flat plate photovoltaic/thermal (PV/T) solar collectors," *Renew. Sustain. Energy Rev.*, vol. 15, no. 1, pp. 352–365, 2011, doi: 10.1016/j.rser.2010.09.024.
- [6] K. O. Adu-Kankam and Luis Camarinha-matos, "Delegating Autonomy on Digital Twins in Energy Ecosystems," *Int. J. SMART GRID*, vol. 6, no. 4, 2022.
- [7] Amar Fahmi Ismail, Ag Sufiyan Abd Hamid, Adnan Ibrahim, Hasila Jarimi, and Kamaruzzaman Sopian, "Performance Analysis of a Double Pass Solar Air Thermal Collector with Porous Media Using Lava Rock," *Energies*, vol. 15, no. 3, 2022, doi: 10.3390/en15030905.
- [8] Hossein Shahinzadeh, Alireza Gheiratmand, Jalal Moradi, and S. Hamid Fathi, "Simultaneous operation of near-to-sea and off-shore wind farms with ocean renewable energy storage," *4th Iran. Conf. Renew. Energy Distrib. Gener. ICREDG 2016*, no. April, pp. 38–44, 2016, doi: 10.1109/ICREDG.2016.7875916.
- [9] K. Sopian, H. T. Liu, S. Kakac, and T. N. Veziroglu, "Performance of a double pass photovoltaic thermal solar collector suitable for solar drying systems," *Energy Convers. Manag.*, vol. 41, no. 4, pp. 353–365, 2000, doi: 10.1016/S0196-8904(99)00115-6.
- [10] Jalal Moradi, Hossein Shahinzadeh, Amirsalar Khandan, and Majid Moazzami, "A profitability investigation into the collaborative operation of wind and underwater compressed air energy storage units in the spot market," *Energy*, vol. 141, pp. 1779–1794, 2017, doi: 10.1016/j.energy.2017.11.088.
- [11] Wan Nur Adilah Wan Roshdan, Hasila Jarimi, Ali H. A. Al-Waeli, Omar Ramadan, and Kamaruzzaman Sopian, "Performance enhancement of double pass photovoltaic/thermal solar collector using asymmetric compound parabolic concentrator (PV/T-ACPC) for façade application in different climates," *Case Stud. Therm. Eng.*, vol. 34, no. February, p. 101998, 2022, doi: 10.1016/j.csite.2022.101998.
- [12] Win Eng Ewe, Ahmad Fudholi, Kamaruzzaman Sopian, Nilofar Asim, Yoyon Ahmudiarto, and Agus Salim, "Overview on Recent PVT Systems with Jet Impingement," *Int. J. Heat Technol.*, vol. 39, no. 6, pp. 1951–1956, 2021, doi: 10.18280/ijht.390633.
- [13] Toshihiko Ishiyama, "Correlation Assessment Between Power Generation and Storage Characteristics by Indoor Photovoltaic Energy Harvesting," vol. 12, no. 4, 2022.
- [14] Marian Kingsley-amaehule, Roland Uhunmwangho, Nkolika Nwazor, and E. Kenneth, "Smart Intelligent Monitoring and Maintenance Management of Photovoltaic Systems," vol. 6, no. 4, 2022.
- [15] Farrukh Javed, "Impact of Temperature & Illumination for Improvement in Photovoltaic System Efficiency," *Int. J. Smart grid*, vol. 6, no. v6i1, 2022, doi: 10.20508/ijsmartgrid.v6i1.222.g185.
- [16] Sébastien A. Brideau and Michael R. Collins, "Experimental model validation of a hybrid PV/thermal air based collector with impinging jets," *Energy Procedia*, vol. 30, pp. 44–54, 2012, doi: 10.1016/j.egypro.2012.11.007.
- [17] Jérôme Barrau, Joan Rosell, Daniel Chemisana, Lounes Tadriss, and M. Ibañez, "Effect of a hybrid jet impingement/micro-channel cooling device on the performance of densely packed PV cells under high concentration," *Sol. Energy*, vol. 85, no. 11, pp. 2655–2665, 2011, doi: 10.1016/j.solener.2011.08.004.
- [18] M. M. K. Bhuiya, M. S. U. Chowdhury, M. Islam, J. U. Ahamed, M. J. H. Khan, M. R. I. Sarker, and M. Saha, "Heat transfer performance evaluation for

- turbulent flow through a tube with twisted wire brush inserts," *Int. Commun. Heat Mass Transf.*, vol. 39, no. 10, pp. 1505–1512, 2012, doi: 10.1016/j.icheatmasstransfer.2012.10.005.
- [19] Mohd Nashrul Mohd Zubir, Mohd Ridha Muhamad, Ahmad Amiri, A. Badarudin, S. N. Kazi, Cheen Sean Oon, Hussein Togun Abdullah, Samira Gharehkhani, and Hooman Yarmand, "Heat transfer performance of closed conduit turbulent flow: Constant mean velocity and temperature do matter!," *J. Taiwan Inst. Chem. Eng.*, vol. 64, pp. 285–298, 2016, doi: 10.1016/j.jtice.2016.04.013.
- [20] Sidi El Bécaye Maïga, Samy Joseph Palm, Cong Tam Nguyen, Gilles Roy, and Nicolas Galanis, "Heat transfer enhancement by using nanofluids in forced convection flows," *Int. J. Heat Fluid Flow*, vol. 26, no. 4 SPEC. ISS., pp. 530–546, 2005, doi: 10.1016/j.ijheatfluidflow.2005.02.004.
- [21] Zi Tao Yu, Xu Xu, Ya Cai Hu, Li Wu Fan, and Ke Fa Cen, "Numerical study of transient buoyancy-driven convective heat transfer of water-based nanofluids in a bottom-heated isosceles triangular enclosure," *Int. J. Heat Mass Transf.*, vol. 54, no. 1–3, pp. 526–532, 2011, doi: 10.1016/j.ijheatmasstransfer.2010.09.017.
- [22] Anja Royne and Christopher J. Dey, "Design of a jet impingement cooling device for densely packed PV cells under high concentration," *Sol. Energy*, vol. 81, no. 8, pp. 1014–1024, 2007, doi: 10.1016/j.solener.2006.11.015.
- [23] Ewe Win Eng., Ahmad Fudholi., Sopian Kamaruzzaman, and Asim Nilofar, "Modeling of bifacial photovoltaic-thermal (PVT) air heater with jet plate," *Int. J. Heat Technol.*, vol. 39, no. 4, pp. 1117–1122, 2021, doi: 10.18280/ijht.390409.
- [24] Ewe Win Eng., Ahmad Fudholi, Kamaruzzaman Sopian, Refat Moshery, Nilofar Asim, Wahidin Nuriana, and Adnan Ibrahim, "Thermo-electro-hydraulic analysis of jet impingement bifacial photovoltaic thermal (JIBPVT) solar air collector," *Energy*, vol. 254, p. 124366, 2022, doi: 10.1016/j.energy.2022.124366.
- [25] Ahmad Fudholi, Muhammad Zohri, Nurul Shahirah Binti Rukman, Nurul Syakirah Nazri, Muslizainun Mustapha, Chan Hoy Yen, Masita Mohammad, and Kamaruzzaman Sopian, "Exergy and sustainability index of photovoltaic thermal (PVT) air collector: A theoretical and experimental study," *Renew. Sustain. Energy Rev.*, vol. 100, no. July 2018, pp. 44–51, 2019, doi: 10.1016/j.rser.2018.10.019.
- [26] Xingshu Sun, Mohammad Ryyan Khan, Chris Deline, and Muhammad Ashraful Alam, "Optimization and performance of bifacial solar modules: A global perspective," *Appl. Energy*, vol. 212, no. December 2017, pp. 1601–1610, 2018, doi: 10.1016/j.apenergy.2017.12.041.
- [27] K. Sopian, K. S. Yigit, H. T. Liu, S. Kakaç, and T. N. Veziroglu, "Performance analysis of photovoltaic thermal air heaters," *Energy Convers. Manag.*, vol. 37, no. 11, pp. 1657–1670, 1996, doi: 10.1016/0196-8904(96)00010-6.